Experimental Neurology 313 (2019) 16–25

Contents lists available at ScienceDirect

Experimental Neurology

journal homepage: www.elsevier.com/locate/yexnr

Research paper

GCN2 reduces inflammation by p-eIF2α/ATF4 pathway after intracerebral hemorrhage in mice

Zhengyang Lu[a,b,1], Zhong Wang[a], Lingyan Yu[b], Yan Ding[b], Yang Xu[b], Ningbo Xu[b], Runnan Li[a], Jiping Tang[b], Gang Chen[a,*], John H. Zhang[b,**]

[a] Department of Neurosurgery, The First Affiliated Hospital of Soochow University, Suzhou, China
[b] Department of Physiology and Pharmacology, Loma Linda University, School of Medicine, Loma Linda, CA, USA

ARTICLE INFO

Keywords:
Intracerebral hemorrhage
Inflammation
General control non-derepressible-2
Inflammsome
Early brain injury

ABSTRACT

Intracerebral hemorrhage (ICH) is a common and severe neurological disorder, which is associated with high rates of mortality and morbidity. This study aimed to evaluate whether general control non-derepressible-2 (GCN2) stimulation ameliorated neuroinflammation after ICH. Male CD-1 mice were subjected to experimental ICH by infusion of bacterial collagenase. Post-ictus assessment included neurobehavioral tests, brain edema measurement, quantification of neutrophil infiltration and microglia activation, and measurement of TNF-α and IL-1β expression at 24 h after ICH. Furthermore, we tested the long-term neurological improvement by GCN2 at 21 days after ICH. Our results showed that GCN2 improved neurological function and reduced brain edema at 24 and 72 h following experimental ICH in CD-1 mice in contrast to the vehicle administration alone. GCN2 was also found to decrease levels of IL-1β and TNF-α, and inhibit neutrophil infiltration activation. In addititon, GCN2 also alleviated long-term neurological impairment after ICH. However, inhibition of eIF2α or ATF4 abolished the protective effects of GCN2, indicating eIF2α/ATF4 signaling pathway as the downstream mediator of GCN2.

1. Introduction

Spontaneous intracerebral hemorrhage (ICH) is one of the deadliest stroke subtypes, accounting for about 15% of all strokes (Sutherland and Auer, 2006; Yang et al., 2016). Yet no specific therapy has been proven clinically effective. There is a general consensus that hemorrhage in the brain leads to tissue disruption and displacement (ADNAN, 2001; Zhai et al., 2016). Hemorrhage is not only directly detrimental to the surrounding brain tissue, but also leads to secondary brain injury, which is characterized by the induction of pro-inflammatory factors, activation of microglia and migration of peripheral inflammatory cells into the center nervous system (Yu et al., 2017; Zhao et al., 2015). Therefore, the anti-inflammatory therapeutic strategy is a promising target for ICH.

General amino acid control non-repressible 2 (GCN2) is a kinase that senses the absence of one or more amino acids by virtue of direct binding to uncharged cognate tRNAs (Ravindran et al., 2013). Decreased consumption of dietary protein leads to the reduction in the amount of amino acids, activation of GCN2, an eventual increase in eIF2α phosphorylation and activation of ATF4(Jung et al., 2015; Laeger et al., 2014). Specifically, GCN2 phosphorylates eukaryotic initiation factor 2 alpha (eIF2α), which attenuates global mRNA translation and then induces a selective subset of stress response genes, for example ATF4. Recent studies demonstrate that the GCN2 kinase plays an important role in reducing inflammation (R et al., 2016). Genetic deletion of GCN2 can result in enhanced intestinal inflammation and Th17-mediated responses, due to elevated IL-1β production (Revelo et al., 2016).

Recently inflammasome, one of the components of the innate immune system, has drawn much attention because of its role in the pathogenesis of sterile inflammatory response by processing caspase-1 and IL-1β to an active stage following human central nervous system disorders (Zhou et al., 2018). Among over 20 NLR members, NLRP3 gains notable attention. It is activated by endogenous stimuli, including

Abbreviations: ICH, Intracrerbral hemorrhage; GCN2, general control non-derepressible-2; eIF2α, eukaryotic initiation factor 2 alpha; ATF4, Activating Transcription Factor 4; i.c.v., intracerebroventricular injuction; i.n, intranasal; MPO, myeloperoxidase

* Correspondence to: G. Chen, Department of Neurosurgery, The First Affiliated Hospital of Soochow University, Suzhou 215000, China.
** Correspondence to: J.H. Zhang, Loma Linda University, 11041 Campus Street, Loma Linda, CA 92350, USA.
E-mail addresses: nju_neurosurgery@163.com (G. Chen), jhzhang@llu.edu (J.H. Zhang).

[1] The first two authors contributed equally to this work.

https://doi.org/10.1016/j.expneurol.2018.12.004
Received 19 August 2018; Received in revised form 11 November 2018; Accepted 4 December 2018
Available online 06 December 2018

uric acid crystals, adenosine triphosphate (ATP), asbestos and silica. Increasing evidence has indicated that GCN2 controls inflammation by inhibiting inflammsome activation (Zhou et al., 2018).

However, to date, no research has investigated the role of GCN2 in ICH models. In this study, we hypothesized that the GCN2 kinase played an important role in controlling inflammation by inhibiting NLRP3 inflammsome though eIF2α/ATF4 pathway after ICH.

2. Materials and methods

All experiments were approved by the Institutional Animal Care and Use Committee of Loma Linda University,

2.1. Animals

All animal procedures for this study were approved by the Institutional Animal Care and Use Committee at Loma Linda University. Eight-week-old male CD-1 mice (weight = 30 g, Charles River, Wilmington, MA) were housed in a 12-h light/dark cycle at a controlled temperature and humidity with unlimited access to food and water. We chose to focus on the male gender in this study since several clinical studies have indicated that male sex could be one of the risk factors for spontaneous ICH (Marini et al., 2017; Roquer et al., 2016). In addition, estrogen has been shown to be protective in ICH (Arbor, 2005; Nakamura et al., 2006). Naïve female mice at this age might not represent a large clinical population.

2.2. ICH model

The general procedures for inducing ICH in the mouse using bacterial collagenase (0.075 U dissolved in 0.5 μl of PBS) into the basal ganglia were performed as described in previous publications (Chen et al., 2018; Ma et al., 2011, 2014). Briefly, mice were anesthetized with ketamine (100 mg/kg, i.p.) and xylazine (10 mg/kg, i.p.) and positioned prone in a stereotaxic head frame. An electronic thermostat-controlled warming blanket was used to maintain the animals' core temperature at 37 °C. The calvarium was exposed by a midline scalp incision from the nasion to the superior nuchal line, and the skin was retracted laterally. With a variable speed drill a 1 mm burr hole was made 0.2 mm posterior to Bregma and 2.2 mm to the right of the midline. A 26-G needle on a Hamilton syringe was inserted with stereotaxic guidance 3.5 mm into the right deep cortex/basal ganglia. The collagenase (0.5 μl) was infused into the brain at a rate of 0.167 μl/min. The needle was left in place for an additional 10 min after injection to prevent the possible leakage of the collagenase solution. After removal of the needle, the incision was closed, and the mice were allowed to recover. The sham operation was performed with needle insertion only.

2.3. Drug administration

GCN2 was purchased form Abcam and it was dissolved in PBS before injection. GCN2 was tested at three different doses (0.5 μg, 1.5 μg and 5.0 μg per mouse), which were administered in the ICH + GCN2 group at 1 h after surgery intranasally. eIF2α and ATF4 small interfering RNA (siRNA), as well as scramble siRNA, were purchased form Origene Technologies, Inc. (MD) and dissolved in sterile RNAse free resuspension buffer according to the manufacturer's instructions. siRNA or scramble RNA (100 pmol) was administered *via* intracerebroventricular injection (i.c.v) at 48 h pre-surgery as previously described.

2.4. Experiment design

Experiment 1: 30 mice were randomly divided in 5 groups (sham, ICH + vehicle, ICH + GCN2 low dosage, ICH + GCN2 medium dosage, ICH + GCN2 high dosage). Recombinant GCN2 was administered intranasally at 3 different dosages (0.15 μg/mouse; 0.5 μg/mouse; 1.5 μg/mouse) at 1 h after ICH. Neurological deficits, brain edema measurement and western blot were performed at 24 h.

Experiment 2: 18 mice were randomly divided in 3 groups (sham, ICH + vehicle, ICH + GCN2 best dosage). Recombinant GCN2 was administered intranasally at 1 h after ICH. Neurological deficits and brain water content were assessed at 72 h after ICH.

Experiment 3: To determine the time course of GCN2 and eIF2α after ICH, Western blot analysis for GCN2, eIF2α and ATF4 expression was performed in the ipsilateral/right hemisphere of each group at 3, 6, 12, 24, 72 h after ICH. 9 mice randomly divided in 3 groups (sham, ICH + vehicle and ICH + GCN2) and these mice euthanized for MPO staining.

Experiment 4: Negative control (scramble) siRNA, eIF2α siRNA or ATF4 siRNA (100 pmol in 2 μl) were injected i.c.v. at 24 h before ICH in sham and ICH animals. Modified Garcia Test, Forelimb Placement Test and Corner Turn Test were performed at 24 h after ICH. Then these mice euthanized for Western blot.

Experiment 5: To determine expression of GCN2 and eIF2α on microglia in the ipsilateral hemisphere after ICH, 4 mice were euthanized for immunofluorescence.

Experiment 6: To test the effects of GCN2 treatment in the long-term neurological function after ICH, neurological function was assessed by water maze and rotarod from 1 week to 3 weeks after the hemorrhage. 18 mice were used in Experiment 6: 6 in sham group, 7 in ICH group and 5 in GCN2 group.

2.5. Neurobehavioral tests

Neurobehavioral outcomes were evaluated by the modified Garcia test for the sensorimotor deficits as previously described (Manaenko et al., 2016; Xie et al., 2018). Three tests were used to evaluate neurological deficits: (1) The modified Garcia Test, in which mice were given a score ranging from 0 to 21. The scoring system consists of seven tests (spontaneous activity, side stroking, vibrissae touch, limb symmetry, lateral turning, forelimb walking and climbing), with possible scores of 0–3 (0 = worst; 3 = best) for each. (2) The limb placement test, in which the animals were held by their trunk positioned parallel to a table top and slowly moved up and down, allowing the vibrissae on one side of the head to brush along the table surface. Refractory placements of the impaired (left) forelimb were evaluated, and a score was calculated as the number of successful forelimb placements out of 10 consecutive trials. (3) Corner Turn Test. Mice were allowed to walk into a 30-degree corner. When exiting the corner, the mouse could turn either to the left or the right, and this choice was recorded. Trials were repeated 10 times and the percentage of left turns was calculated.

Animals were numbered and randomized into different experimental groups using Excel. The scientists who did the neurobehavioral tests and data analysis were blinded to the experimental group of each animal. Animals were uncoded after the analysis.

2.6. Morris water maze

Between days 7 and 21 following ICH, the Morris water maze test was performed in a blinded setup to evaluate ICH-induced neurocognitive deficits, as previously described (Liao et al., 2016), Briefly, the test consisted of three trials, including a cued learning paradigm, spatial paradigm and probe paradigm. All trials lasted a maximum of 60 s.

The cued learning trials were conducted on Day 18 after ICH for non-associative factors that could affect scoring on the Morris water maze, such as motivation, swimming ability and vision. During the cued learning trials, there was a visible platform above the water surface. Mice were placed in the tank, required simply to swim to the platform by the end of each trial and were allowed to remain on the platform for 10 s after finding or being guided to it.

On the following 3 consecutive days, the spatial and probe trials

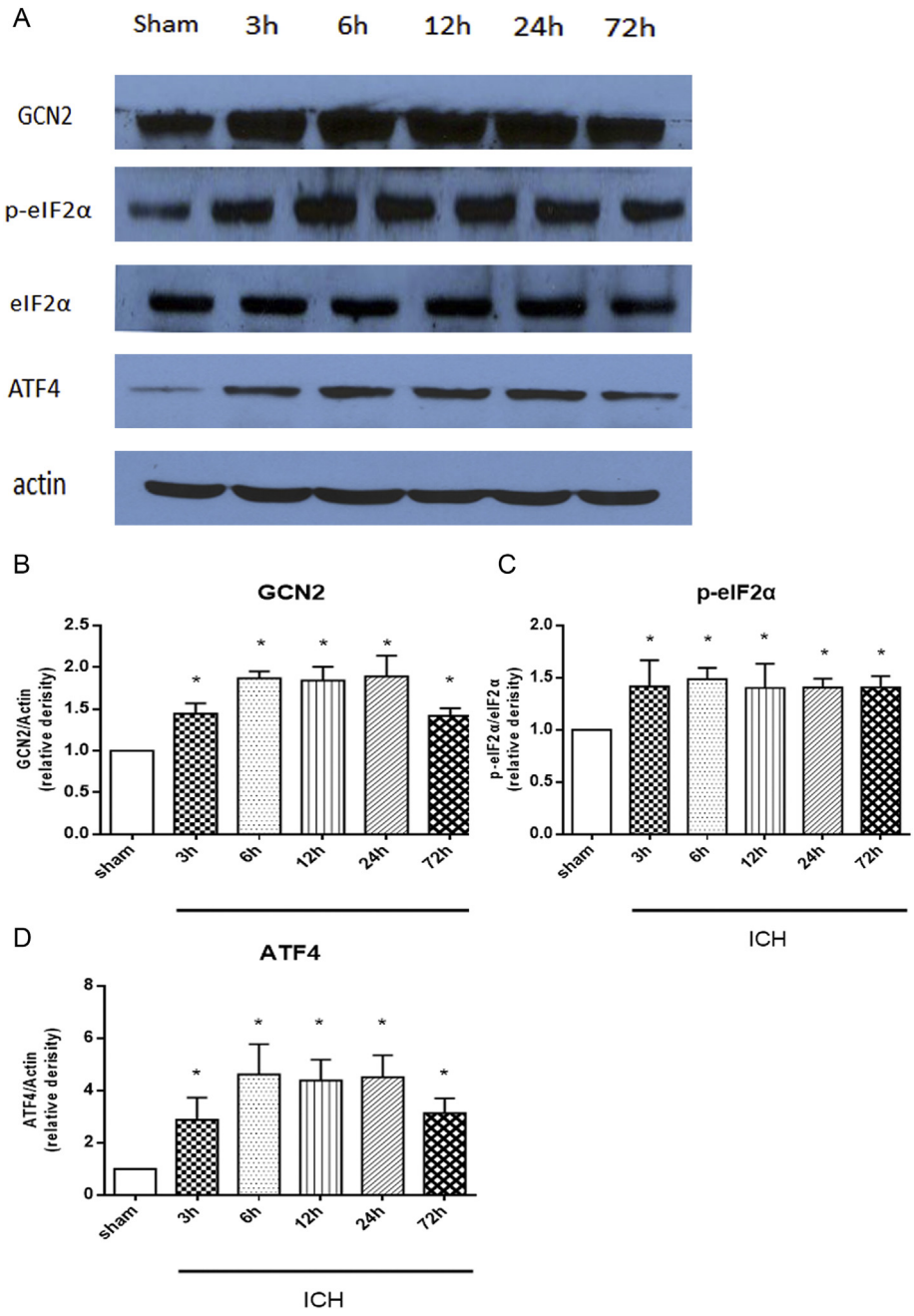

Fig. 1. Time course expression of GCN2, p-eIF2α, total eIF2α and ATF4 by Western blot. N = 6 mice/group. *p < .05 vs sham.

were conducted to measure the ability of the mouse to learn and remember the location of a hidden platform in the tank. Unlike the cued learning trial, the platform in these trials was submerged under the water. Once a mouse was released in the tank, it was allowed to swim and search for the platform. The total distance to find the platform was measured to reflect spatial learning ability. At 1 h after the spatial trial, the platform was removed completely and the mice were allowed to swim again in search of the now-absent platform. The percentage of time spent in the probe quadrant (the previous location of the platform) was measured to reflect spatial memory ability.

2.7. Rotarod test

The rotarod test was performed at the first-, and third-week post-ICH to assess sensorimotor coordination and balance as previously described (Zhou et al., 2018). The mice were placed on an accelerating horizontal cylinder and the latency and rotational speed of each subject's falling off was recorded by a blinded evaluator. Three constant velocity runs of 1 min each were done per subject prior to testing. Three scoring trials were performed at each of 5 or 10 rpm starting speeds with regular increases in velocity, with the mean averages of falling latency used for comparison.

2.8. Brain water content

Brain water content was evaluated as previously reported (Manuscript, 2015; Yang et al., 2016). Briefly, mice were decapitated under deep anesthesia. Brains were immediately removed and cut into 4 mm sections around the needle track. Each section was divided into four parts: ipsilateral and contralateral basal ganglia, ipsilateral and contralateral cortex. The cerebellum was collected as control. Each part was weighed on an electronic analytical balance and then dried at

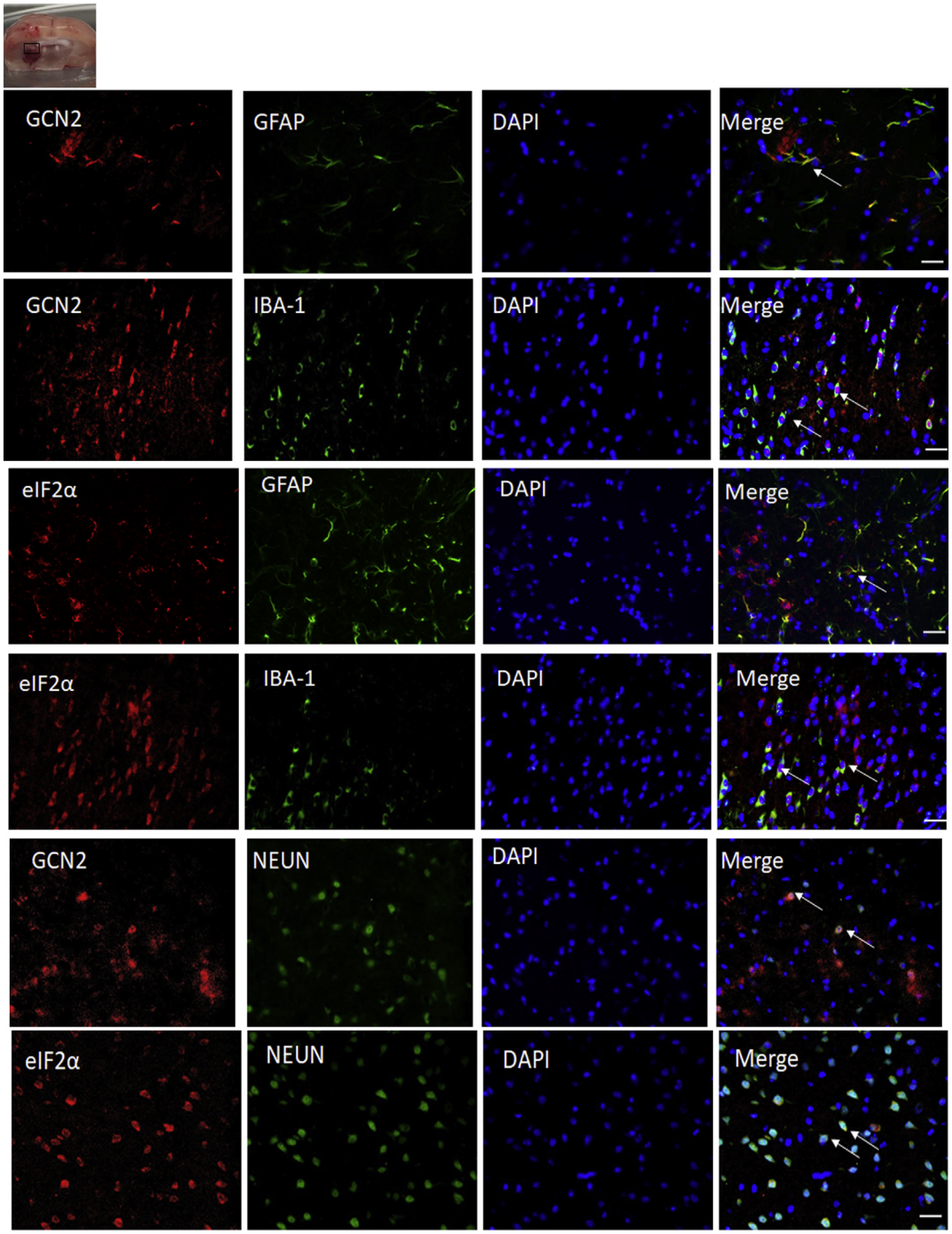

Fig. 2. Immunostaining of GCN2 and eIF2α with IBA-1(microgia), GFAP (astrocytes), and NeuN (neurons) at 24 h after ICH. Scale bar = 50 μm.

100 °C for 24 h to determine the dry weight (DW). Brain water content (%) was calculated as [(WW − DW) / WW] × 100.

2.9. Western blot analysis

Brain sample were collected at 24 h after ICH. Mice were perfused transcardially with 40 ml PBS, and proteins of the ipsilateral hemispheres were extracted by homogenizing in RIPA buffer (Santa Cruz Biotechnology). Western blotting was performed as previously described (Xie et al., 2018; Zhou et al., 2018). The primary antibodies included anti-GCN2(1:500; Santa Cruz Biotechnology, Santa Cruz, CA), anti-eIF2α (Santa Cruz Biotec hnology, Santa Cruz, CA), anti-p-eIF2α (Santa Cruz Biotechnology, Santa Cruz, CA), anti-ATF4(Abcam, Cambridge, MA), anti-NLRP3(Abcam, Cambridge, MA), anti-IL-1β (Santa Cruz Biotechnology, Santa Cruz, CA), anti-TNFα (Abcam, Cambridge, MA), anti-MPO (Abcam, Cambridge, MA) and β-actin (Santa Cruz Biotechnology, Santa Cruz, CA).

2.10. Immunohistochemistry staining

Immunohistochemistry staining for brain was performed on fixed frozen section as previously described (Yang et al., 2016),with primary antibodies: anti-GCN2 (Santa Cruz Biotechnology, Santa Cruz, CA); anti-eIF2α (Santa Cruz Biotechnology, Santa Cruz, CA), anti-GFAP (Abcam, Cambridge, MA), anti-Iba-1(Abcam, Cambridge, MA), and anti-NeuN (Abcam, Cambridge, MA), The slides were viewed and

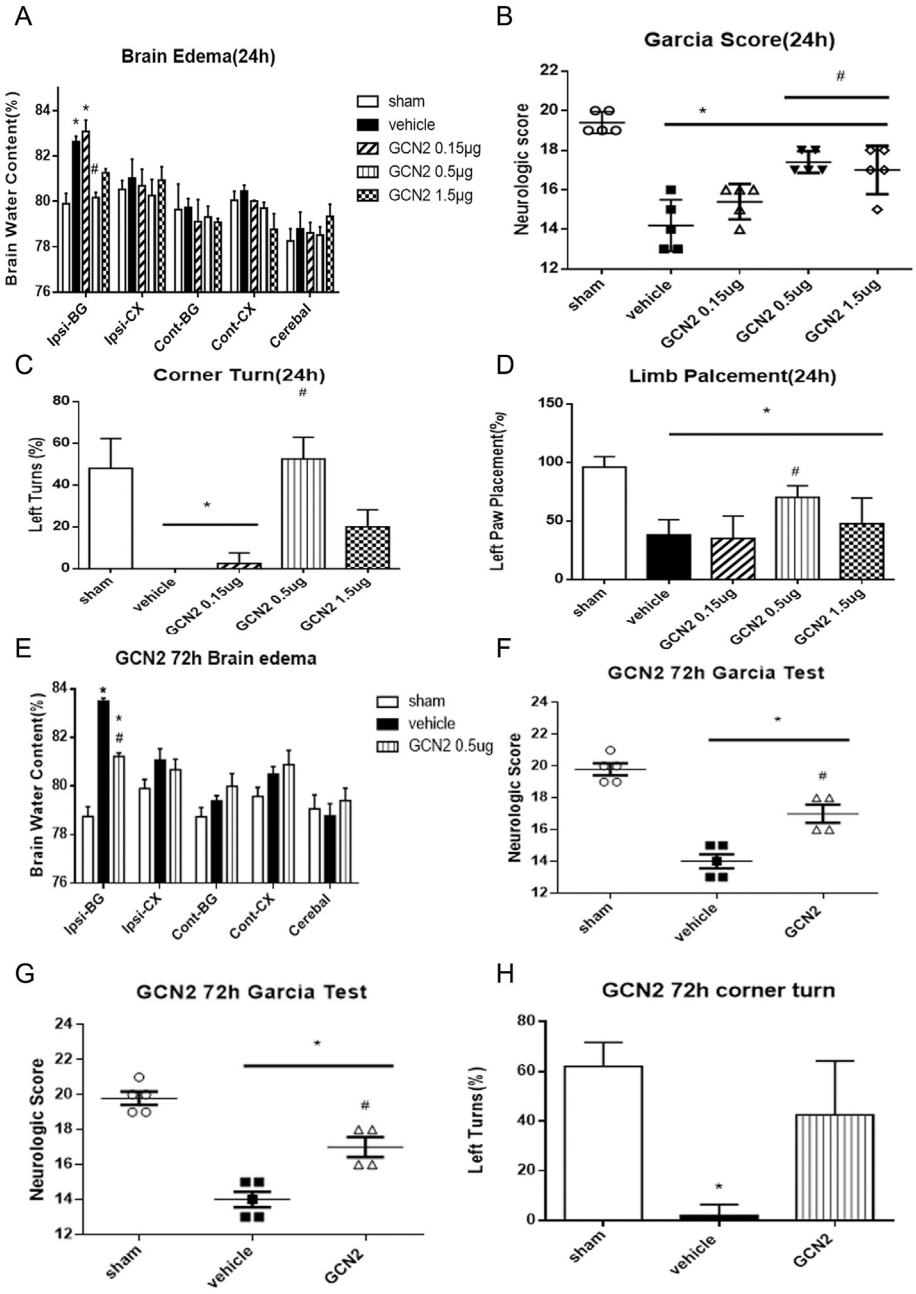

Fig. 3. Administration of GCN2 decreased brain water content and improved neurobehavioral performance at 24 h after intracerebral hemorrhage (ICH). (A) Brain water content; (B) Modified Garcia test; (C) Limb placement test, and (D) Corner turn test. Administration of GCN2 also decreased brain water content and improved neurobehavioral performance at 72 h after ICH at best dosage. N = 5 mice/group. *p < .05 vs. sham, *p < .05 vs. ICH + vehicle. Values are expressed as mean ± SD.

images were taken using LAS X software with a Leica DMi 8 fluorescence microscope (Leica Microsystems, Germany).

2.11. Statistical analysis

In this exploratory study, all data were expressed as mean ± SD and all tests were done two-sided. Before statistical tests, normal distribution and similar variation between experimental groups were inspected for appropriateness. We analyzed the data by using one-way ANOVA with Tukey's post-hoc test and Kruskall-Wallis with Dunn's post-hoc tests was used for non-parametric data. P values of < 0.05 were considered statistically significant. On the basis of the results of the pilot preliminary study for neurobehavioral function and brain water content, six mice were required to achieve 90% power to detect a difference, with a probability of p < .05 . GraphPad Prism 6 and SPSS18. 0 were us ed. for graphing and analyze all data.

3. Results

3.1. GCN2 and phosphorylated EIF2α expression levels were upregulated following ICH injury

We first investigated whether GCN2 and phosphorylated eIF2α levels would change in response to the brain injury following ICH. The Western blot results showed that GCN2 level was significantly increased as early as 3 h after ICH, reached a peak at 24 h and then declined at 72 h (Fig. 1B) (P < .05). Similarly, phoshphorylated eIF2α was significantly increased at 3 h, peaked at 6 h and remained at a high level

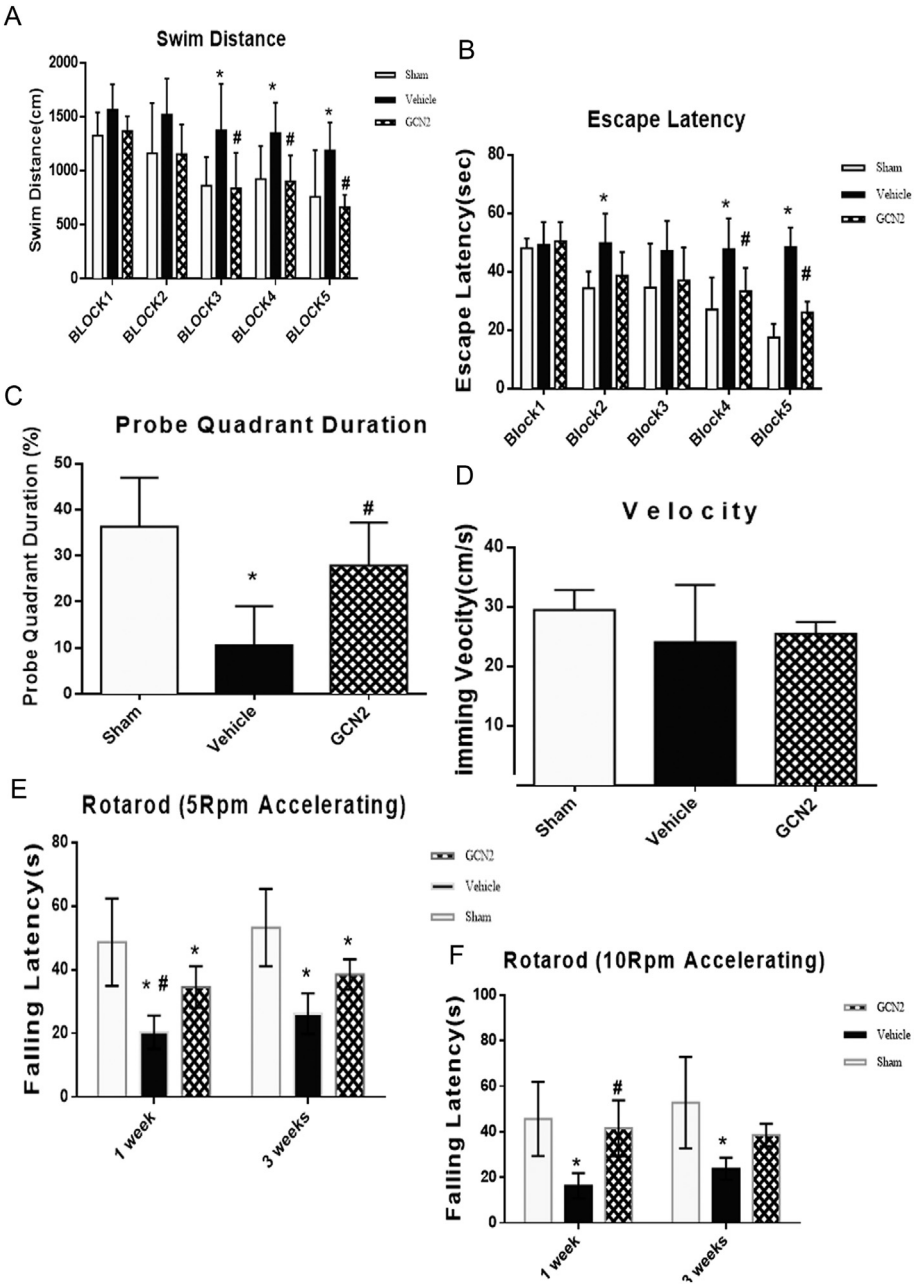

Fig. 4. Administration of GCN2 improved long-term neurological function at four weeks post-ICH. GCN2 treatment group showed significant memory function recovery compared to the vehicle group in reduced swimming distance to platform (A), reduced escape latency (B), and more time spent in the target quadrant during the probe phase (C). But there is no significant difference in speed. GCN2-treated animals had significantly better rotarod performance than vehicle mice at 1 week, but not at 3 weeks (E,F).n = 8–10 mice/group.

(Fig. 1C) ($P < .05$). Meanwhile, we also detected the expression of ATF4 in the brain. The result of Western blot showed that ATF4 protein level increased at 3 h after ICH, reached to peak at 6 h, remained at a high level form 6 h to 24 h and decreased at 72 h after ICH (Fig. 1D) ($P < .05$) (Fig. 1). Immunofluorescence staining revealed that the GCN2 and eIF2α were expressed on microglia, astrocytes and neurons. (Fig. 2).

3.2. GCN2 treatment improved neurobehavioral outcomes in short-term and long-term, reduced brain water content both at 24, 72 h after ICH and neutrophil infiltration

The results at 24 and 72 h showed that ICH animals demonstrated severe deficits compared to sham animals in the modified Garcia test as well as increased perihematomal brain water content in the ipsilateral basal ganglia (Fig. 3A,B,C,D). GCN2 was administered at 1 h after ICH. At 24 h, the medium-dosage group improved significantly than the vehicle group in neurobehavioral tests and brain water content were also significantly reduced ($P < .05$) (Fig. 3A,B,C,D). Based on these results, we chose the medium dosage as the best treatment to test neurobehavioral function and brain edema at 72 h post-ICH. The results showed that GCN2 could significantly improve neurological function and that brain edema in the ipsilateral basal ganglia (ipsi-BG) was also significantly reduced compared to the ICH group ($P < .05$) (Fig. 3E,F,G,H).

Based on the results above, we chose the best dosage for the long-term study. In the Rotarod test, the ICH + vehicle group had significantly shorter latency to fall compared with the sham group both in

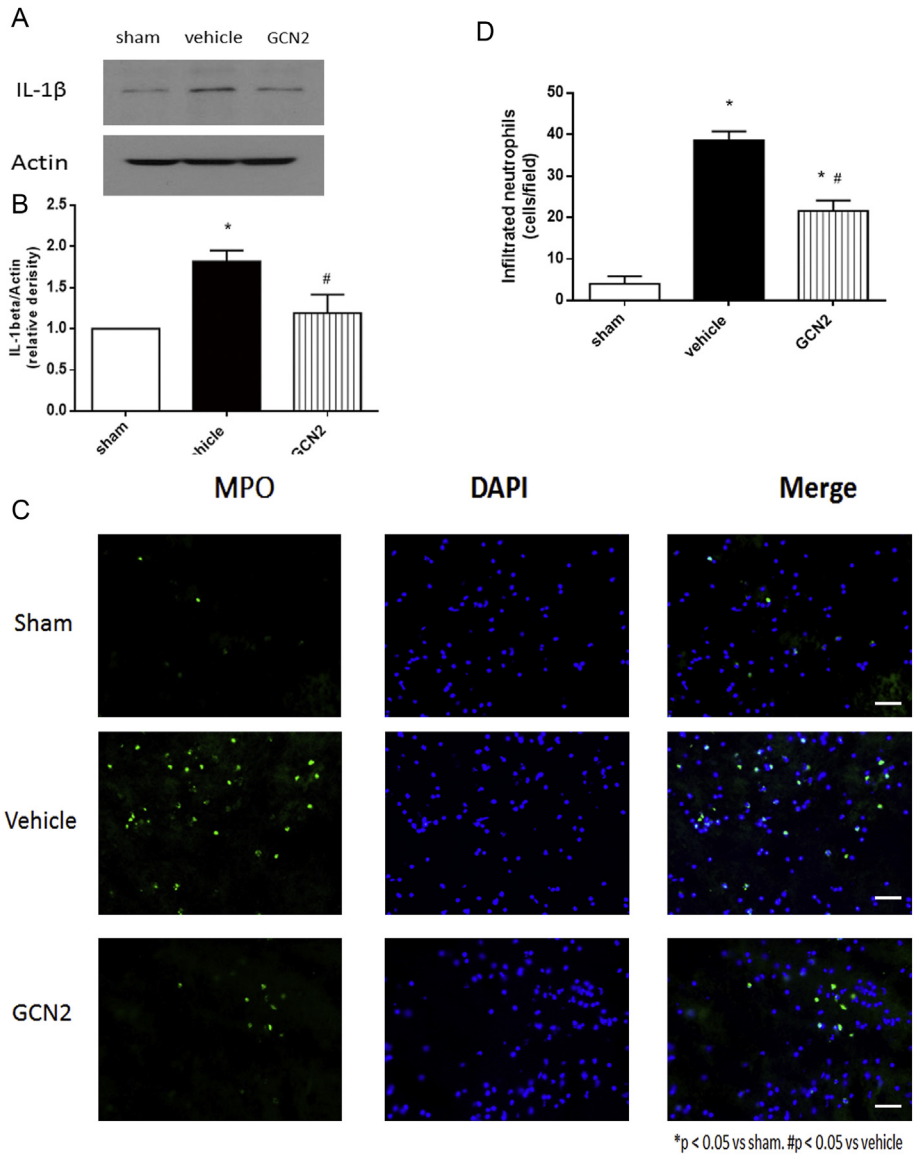

Fig. 5. Administration of GCN2 reduced neutrophil infiltration at 24 h after ICH. This result showed that administration of GCN2 could inhibit activity of MPO effectively (C,D). IL-1β levels significantly decreased after GCN2 treatment (A,B).
MPO = myeloperoxidase. Scale bar = 50 μm. n = 6/group.

the 5 revolution per minute (RPM) and 10RPM accelerating velocity tests on 1 week and 3 weeks. One week after ICH, GCN2 significantly improved performance in the 5 RPM and 10 RPM tests ($P < .05$) (Fig. 4E,F). Three weeks after ICH, there was no significant different between the ICH + vehicle group and ICH + GCN2 group ($P < .05$, Fig. 4E,F). In water maze test, GCN2 treatment showed significant memory function recovery compared to the vehicle-treated group in reduced swimming distance (Fig. 4A) to platform, reduced escape latency (Fig. 4B), and spent more time in the target quadrant during the probe phase (Fig. 4C). But there was no difference in swimming velocity among three groups, indicating that the difference in latency was due to the impaired memory, instead of swimming ability ($P < .05$) (Fig. 4D).

We tested IL-1β by Western blot. The results showed that IL-1β levels significantly decreased after GCN2 treatment ($P < .05$) (Fig. 5A,B).

Meanwhile, we detected myeloperoxidase (MPO) levels in brain tissue by immunostaining at 24 h following ICH to determine the effect of GCN2 on neutrophil infiltration. The immunostaining results showed that after GCN2 treatment the number of MPO-positive cells in the perihematomal area significantly reduced compared to ICH group (Fig. 5C,D).

3.3. eIF2α and ATF4 knockdown reversed the anti-inflammatory effect of GCN2

eIF2α *in vivo* knockdown were preformed to investigate the potential role of eIF2α in the protective effects of GCN2 activation. We administrated eIF2α siRNA and ATF4 siRNA 24 h before ICH, respectively, followed by the treatment of GCN2 at 24 h after ICH. Western blots results showed that there was a dramatic loss of phosphorylated eIF2α ($P < .05$, Fig. 6B) and that IL-1β increased in ipsilateral brain tissue compared to GCN2 treatment group with or without scramble siRNA ($P < .05$) (Fig. 6F). ATF4 siRNA also abolished the effects of GCN2, as demonstrated by increased IL-1β and TNF-α levels and worse neurological outcomes ($P < .05$) (Fig. 6E,F). These data suggested that GCN2 decreased inflammation dependent on eIF2α and ATF4.

4. Discussion

ICH is a fatal stroke subtype, and increasing evidence shows that

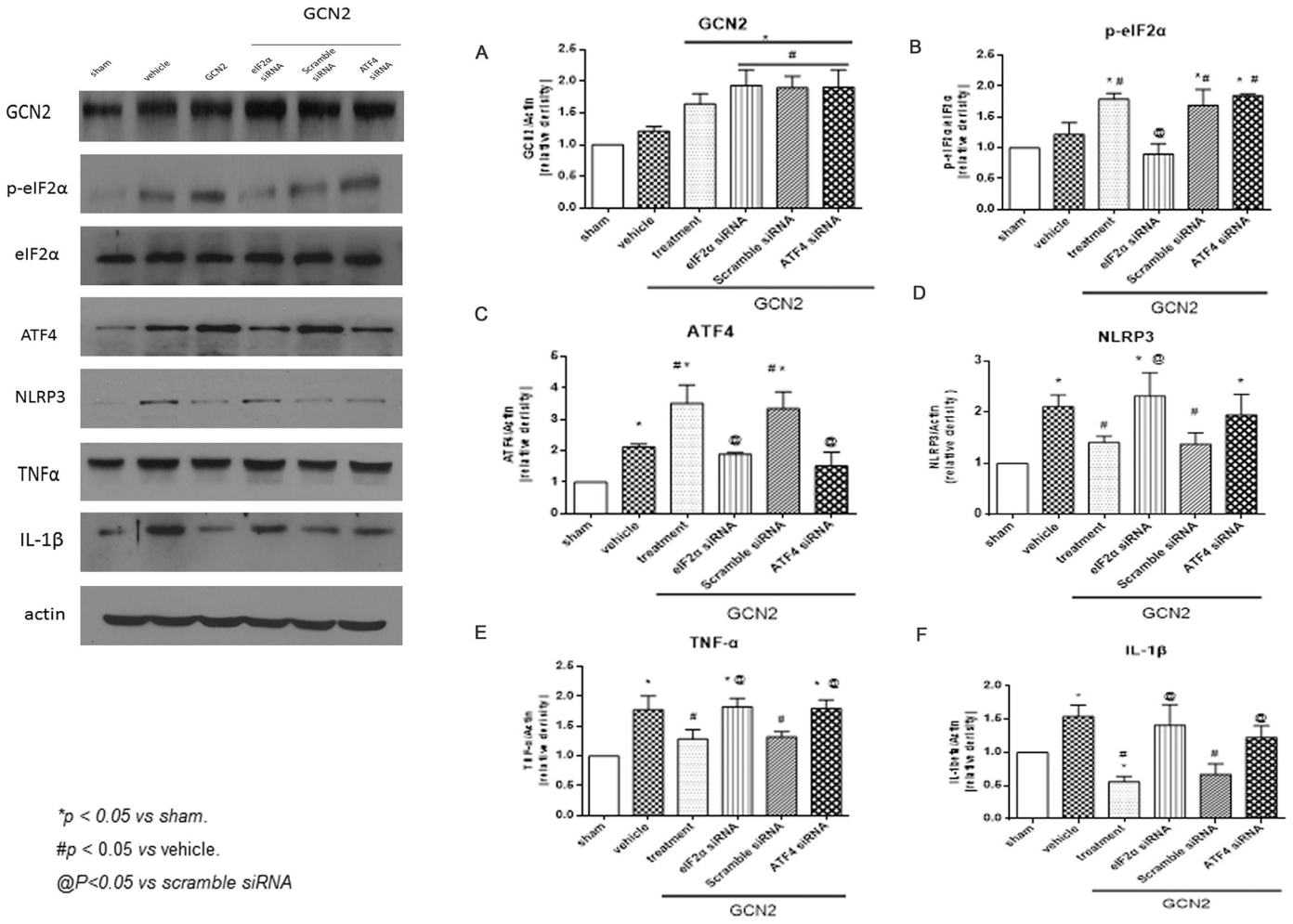

Fig. 6. Effects of GCN2, eIF2α siRNA, and ATF4 siRNA on the expression of GCN2, p-eIF2α, ATF4, NLRP3, TNF-α and IL-1β after ICH. Administration of GCN2 increased protein level of p-eIF2α (B), ATF4 (C) but decreased NLRP3 (D), TNF-α (E), and IL-1β (F). Silencing eIF2α by siRNA reduced the expression of ATF4 (C) and abolished the effect of GCN2 on NLRP3 (D). Silencing ATF4 by siRNA reduced the expression of ATF4 (C), and also abolished the effect of GCN2 on inflammasome (D). n = 6 mice/group. * p < .05 vs. sham, #p < .05 vs. ICH + vehicle, @p < .05 vs. Scramble siRNA.

inflammation plays a critical role in the pathophysiology of ICH-induced brain injury (Ma et al., 2014; Wang and Doré, 2007). This study provided evidence for a molecular pathway activated by GCN2 in ameliorating inflammation following ICH. In the present study, we demonstrated that 1) after ICH, GCN2 increased in the acute phase; 2) GCN2 attenuated neutrophil infiltration, resulting in decrease of TNF-α and IL-1β production, as well as in reduction of neurological deficits and brain edema after ICH. We also tested the effect of GCN2 in the long-term study. The results showed that GCN2 could improve the neurological function.

Accumulating evidence suggests that GCN2 deletion in myeloid cells has a significant effect on systemic autoimmunity, accelerating immune dysfunction and exacerbating outcomes. This is consistent with the role of GCN2 in regulating myeloid inflammatory activity (Ravishankar et al., 2015). Additionally, there is higher production of pro-IL-1β in the colonic macrophages and dendritic cells isolated form GCN2 deletion mice in the large and small intestine (Ravindran et al., 2013). Some evidence demonstrated a clear role for inflammasome activation in mediating the enhanced inflammation in GCN2 deletion mice (Ravindran et al., 2013). Recent research also demonstrated that activation of GCN2 suppressed proinflammatory cytokine production in glomeruli and reduced macrophage recruitment to the kidney during the incipient stage of Ab-induced glomerular inflammation.

Recently, some research indicated that GCN2 controls the infiltration of T cells into inflamed central nervous system following acute autoimmune neuroinflammation (Ravindran et al., 2013). The absence of experimental autoimmune encephalomyelitis remission in GCN2-deficient mice is associated increased expression of Th17-related cytokines and decreased expression of IL-10 in the central nervous system (Ravindran et al., 2013). However, effect of GCN2 in ICH has not been studied so far.

In the present study, we showed that GCN2 and eIF2α were expressed on microglia and increased as early as 3 h after ICH. Moreover, we demonstrated that GCN2 administration into the brains of ICH mice significantly decreased TNF-α and IL-1β levels. The result demonstrated that GCN2 could alleviate neurological deficits. The MPO staining and Western blot results showed that GCN2 treatment can decrease the infiltration of neutrophile granulocytes. These results confirmed our hypothesis that GCN2 suppressed inflammation induced by ICH. In the next part of our study, we investigated the role of NLRP3 inflammasome in the protective effect of GCN2 in ICH-mediated inflammation. Recent evidence has alluded to the notion that a multiple-protein complex, inflammasome, is the major source of IL-1β. The NLRP3 inflammasome belongs to the NLR family, and is associated with the apoptosis-associated speck-like protein containing a caspase recruitment domain (ASC), which recruits and activates caspase-1, therefore releasing cleaved IL-1β (Ma et al., 2014; Ravindran et al., 2013). It has been determined that the NLRP3 inflammasome contributes to ICH-induced inflammatory response (Ma et al., 2014). Unlike other inflammasomes, the NLRP3 inflammasome exhibited its functionality in both sterile

inflammatory response and antimicrobial response. In our experiment, after GCN2 treatment, the NLRP3 inflammsome levels decreased significantly according to our Western blot results. It suggested that GCN2 attenuated NLRP3 inflammsome effectively.

Next, we examined the possible mechanism by which GCN2 attenuated NLRP3 inflammsome. Evidence provided that GCN2 promoted eIF2α phosphorylation response that includes protein synthesis attenuation and an increase in the expression of ATF4(Ma et al., 2014; Ravindran et al., 2013). Based on our results that GCN2 could attenuate NLRP3 inflammasome, we put forward a hypothesis that GCN2 attenuates NLRP3 inflmmasome by eIF2α/ATF4 pathway. So we knocked down eIF2α and ATF4 by siRNA, respectively, and the results of Western bolt showed that after eIF2α or ATF4 was inhibited, NLRP3 levels increased significantly, which verified our hypothesis.

There are some limitations in this study. First, the direct relationship between GCN2 and ICH has not been studied. The exact mechanism by which ICH influenced the level of GCN2 remains to be discovered. Second, we only focused on the effect of GCN2 on inflammation after ICH. We did not explore the physiology role of GCN2 in blood-brain barrier function, anti-apoptotic pathway or other neuroprotective effects of GCN2 after ICH. Additionally, we only tested three doses and one route of administration at a one time point. To enhance the translatability of the study, we would need to explore other treatment regimens, as well as the outcomes at other time points. Thus future studies are needed to investigate the other protective functions, as well as signaling mechanisms.

In conclusion, the present study indicates that GCN2 level increased after ICH in brain tissues, and that exogenous GCN2 could improve neurological outcomes and decrease brain water content. This protective effect was by inhibiting NLRP3 *via* eIF2α/ATF4 signaling pathway. This study could possibly provide a potential novel treatment for ICH.

Ethics approval

Humans were not used in this study.

All animals` experiments were approved by the Loma Linda University Institutional Animal Care and Use Committee.

Consent for publication

No.

Availability of data and materials

The authors confirm that all data underlying the findings are fully available without restriction. All relevant data are within the paper and its supporting information files.

Declaration of conflicting interests

The author(s) declared no potential conflicts of interest with respect to the research, authorship, and/or publication of this article.

Akcnowledgements

Zhengyang Lu and Zhong Wang conceived and designed the study. Lingyan Yu, Yang Xu and Xue Li did the experimental design and collected the data. Runnan Li and Ningbo Xu contributed to analyzing the data. Yan Ding provided language help and writing assistance. John H. Zhang, Gang Chen and Jiping Tang conceived, designed and coordinated the study.

References

Adnan, Q.U., 2001. Spontaneous intracerebral hemorrhage. N. Engl. J. Med. Rev. 344, 1450–1460.

Arbor, A., 2005. Estrogen Therapy for Experimental Intracerebral Hemorrhage in Rats. 103. pp. 97–103.

Chen, S., Zhao, L., Sherchan, P., Ding, Y., Yu, J., Nowrangi, D., Tang, J., Xia, Y., Zhang, J.H., 2018. Activation of melanocortin receptor 4 with RO27-3225 attenuates neuroinflammation through AMPK/JNK/p38 MAPK pathway after intracerebral hemorrhage in mice. J. Neuroinflammation 15, 1–13.

Jung, J.G., Yi, S.-A., Choi, S.-E., Kang, Y., Kim, T.H., Jeon, J.Y., Bae, M.A., Ahn, J.H., Jeong, H., Hwang, E.S., Lee, K.-W., 2015. TM-25659-Induced Activation of FGF21 Level Decreases Insulin Resistance and Inflammation in Skeletal Muscle via GCN2 Pathways. Mol. Cells 38, 1037–1043.

Laeger, T., Henagan, T.M., Albarado, D.C., Redman, L.M., Bray, G.A., Noland, R.C., Münzberg, H., Hutson, S.M., Gettys, T.W., Schwartz, M.W., Morrison, C.D., 2014. FGF21 is an endocrine signal of protein restriction. J. Clin. Invest. 124, 3913–3922.

Liao, F., Li, G.F., Yuan, W., Chen, Y.J., Zuo, Y.C., Rashid, K., Zhang, J.H., Feng, H., Liu, F., 2016. LSKL peptide alleviates subarachnoid fibrosis and hydrocephalus by inhibiting TSP1-mediated TGF-beta 1 signaling activity following subarachnoid hemorrhage in rats. Exp. Ther. Med. 12, 2537–2543.

Ma, Q., Huang, B., Khatibi, N., Rolland, W., Suzuki, H., Zhang, J.H., Tang, J., 2011. PDGFR-α inhibition preserves blood-brain barrier after intracerebral hemorrhage. Ann. Neurol. 70, 920–931.

Ma, Q., Chen, S., Hu, Q., Feng, H., Zhang, J.H., Tang, J., 2014. NLRP3 inflammasome contributes to inflammation after intracerebral hemorrhage. Ann. Neurol. 33, 395–401.

Manaenko, A., Yang, P., Nowrangi, D., Budbazar, E., Hartman, R.E., Obenaus, A., Pearce, W.J., Zhang, J.H., Tang, J., 2016. Inhibition of Stress Fiber Formation Preserves Blood – Brain Barrier after Intracerebral Hemorrhage in Mice. https://doi.org/10.1177/0271678X16679169.

Manuscript, A., 2015. Edema in Two Mouse Models of Intracerebral Hemorrhage. pp. 151–160. https://doi.org/10.1016/j.bbr.2014.01.052.Correlation.

Marini, S., Morotti, A., Ayres, A.M., Crawford, K., Kourkoulis, C.E., Lena, U.K., Gurol, E.M., Viswanathan, A., Goldstein, J.N., Greenberg, S.M., Biffi, A., Rosand, J., Anderson, C.D., 2017. Sex differences in intracerebral hemorrhage expansion and mortality. J. Neurol. Sci. 379, 112–116.

Nakamura, T., Xi, G., Keep, R.F., Wang, M., Nagao, S., Hoff, J.T., Hua, Y., 2006. Effects of endogenous and exogenous estrogen on intracerebral hemorrhage-induced brain damage in rats. Acta Neurochir. Suppl. 218–221. https://doi.org/10.1007/3-211-30714-1-47.

R, R., J, L., Hi, N., N, K., H, M., L, G., D, M., B, L., P, H., Y, W., S, L., Pa, S., 2016. The amino acid sensor GCN2 controls gut inflammation by inhibiting inflammasome activation Rajesh. Nature 21, 4062–4072.

Ravindran, R., Khan, N., Nakaya, I.H., Li, S., Loebbermann, J., Maddur, Mohan S., Park, Y., Jones, D.P., David, Ron, Davoust, J., David, W., Herbert, V., David, R., Bali, P., 2013. Vaccine activation of the nutrient sensor GCN2 in dendritic cells enhances antigen presentation. Science 2, 1–8.

Ravishankar, B., Liu, H., Shinde, R., Chaudhary, K., Xiao, W., Bradley, J., Koritzinsky, M., Madaio, M.P., McGaha, T.L., 2015. The amino acid sensor GCN2 inhibits inflammatory responses to apoptotic cells promoting tolerance and suppressing systemic autoimmunity. PNAS 201504276. https://doi.org/10.1073/pnas.1504276112.

Revelo, X.S., Winer, S., Winer, D.A., 2016. Starving Intestinal Inflammation with the Amino Acid Sensor GCN2. Cell Metab. 23, 763–765.

Roquer, J., Rodriguez-Campello, A., Jimenez-Conde, J., Cuadrado-Godia, E., Giralt-Steinhauer, E., Vivanco Hidalgo, R.M., Soriano, C., Ois, A., 2016. Sex-related differences in primary intracerebral hemorrhage. Neurology 87, 257–262.

Sutherland, G.R., Auer, R.N., 2006. Primary intracerebral hemorrhage. J. Clin. Neurosci. 13, 511–517.

Wang, J., Doré, S., 2007. Inflammation after intracerebral hemorrhage. J. Cereb. Blood Flow Metab. 27, 894–908.

Xie, Z., Huang, L., Enkhjargal, B., Reis, C., Wan, W., Tang, J., Cheng, Y., Zhang, J.H., 2018. Recombinant Netrin-1 binding UNC5B receptor attenuates neuroinflammation and brain injury via PPARγ/NFκB signaling pathway after subarachnoid hemorrhage in rats. Brain Behav. Immun. 69, 190–202.

Yang, P., Manaenko, A., Xu, F., Miao, L., Wang, G., Hu, X., Guo, Z.N., Hu, Q., Hartman, R.E., Pearce, W.J., Obenaus, A., Zhang, J.H., Chen, G., Tang, J., 2016. Role of PDGF-D and PDGFR-β in neuroinflammation in experimental ICH mice model. Exp. Neurol. 283, 157–164.

Yu, A., Zhang, T., Zhong, W., Duan, H., Wang, S., Ye, P., Wang, J., Zhong, S., Yang, Z., 2017. miRNA-144 induces microglial autophagy and inflammation following intracerebral hemorrhage. Immunol. Lett. 182, 18–23.

Zhai, W., Chen, D., Shen, H., Chen, Z., Li, H., Yu, Z., Chen, G., Rodriguez-Yanez, M., Castellanos, M., Freijo, M., Fernandez, J.L., Marti-Fabregas, J., Nombela, F., Asch, C., Luitse, M., Rinkel, G., Tweel, I., Algra, A., Klijn, C., Cannon, J., Xi, G., Keep, R., Qureshi, A., Mendelow, A., Hanley, D., Schlunk, F., Greenberg, S., Qureshi, A., Tuhrim, S., Broderick, J., Batjer, H., Hondo, H., Hanley, D., Behrouz, R., Gebel, J., Jauch, E., Brott, T., Khoury, J., Sauerbeck, L., Salisbury, S., Gebel, J., Jauch, E., Brott, T., Khoury, J., Sauerbeck, L., Salisbury, S., Qureshi, A., Ling, G., Khan, J., Suri, M., Miskolczi, L., Guterman, L., Xiong, X., Yang, Q., Chen, S., Yang, Q., Chen, G., Zhang, J., Hua, Y., Nakamura, T., Keep, R., Wu, J., Schallert, T., Hoff, J., Lee, S., Chu, K., Sinn, D., Jung, K., Kim, E., Kim, S., Zhang, Y., Lautt, W., Correia-De-Sa, P., Ribeiro, J., Lindquist, B., Shuttleworth, C., Durmaz, R., Ozkara, E., Kanbak, G., Arslan, O., Dokumacioglu, A., Kartkaya, K., Chen, J., Sonsalla, P., Pedata, F., Melani, A., Domenici, M., Popoli, P., Lin, C., Dumont, A., Tsai, Y., Huang, J., Chang, K., Kwan, A., Lin, C., Su, Y., Dumont, A., Shih, H., Lieu, A., Howng, S., Schulte, G., Fredholm, B., Dickenson, J., Blank, J., Hill, S., Seidel, M., Klinger, M., Freissmuth, M., Holler, C., Sexl, V., Mancusi, G., Holler, C., Gloria-Maercker, E., Schutz, W., Freissmuth, M., Gao, Z., Chen, T., Weber, M., Linden, J., Brust, T., Cayabyab, F., Zhou, N., MacVicar, B., Chen, Z., Xiong, C., Pancyr, C., Stockwell, J., Walz, W., Cayabyab, F., Kenakin, T.,

Jeong, H., Jou, I., Joe, E., Lee, H., Kim, M., Jan, M., Penn, R., Emala, C., Aronowski, J., Zhao, X., Jeong, H., Ji, K., Kim, B., Kim, J., Jou, I., Joe, E., Zimmermann, H., Zebisch, M., Strater, N., Chen, J., Zhao, Y., Liu, Y., Junger, W., Lin, C., Shih, H., Lieu, A., Lee, K., Dumont, A., Kassell, N., Sehba, F., Flores, R., Muller, A., Friedrich, V., Chen, J., Britz, G., Kim, M., Chen, S., Park, S., Kim, M., D'Agati, V., Yang, J., Leshem-Lev, D., Hochhauser, E., Chanyshev, B., Isak, A., Shainberg, A., Nayak, G., Prentice, H., Milton, S., Yang, T., Gao, X., Sandberg, M., Zollbrecht, C., Zhang, X., Hezel, M., Tofovic, S., Salah, E., Smits, G., Whalley, E., Ticho, B., Deykin, A., Carroll, R., Yellon, D., Why, S., Mann, A., Ardito, T., Thulin, G., Ferris, S., Macleod, M., Huot, J., Houle, F., Marceau, F., Landry, J., Concannon, C., Orrenius, S., Samali, A., Concannon, C., Gorman, A., Samali, A., Zhao, L., Liu, X., Liang, J., Han, S., Wang, Y., Yin, Y., Wu, H., Wu, T., Li, M., Wang, J., Wang, J., Fields, J., Zhao, C., Langer, J., Thimmulappa, R., Kensler, T., Nascimento, F., Figueredo, S., Marcon, R., Martins, D., Macedo, S., Lima, D., Rosim, F., Persike, D., Nehlig, A., Amorim, R., Oliveira, D., Fernandes, M., Mayne, M., Fotheringham, J., Yan, H., Power, C., Bigio, M., Peeling, J., 2016. A1 adenosine receptor attenuates intracerebral hemorrhage-induced secondary brain injury in rats by activating the P38-MAPKAP2-Hsp27 pathway. Mol. Brain 9, 66.

Zhao, X., Wu, T., Chang, C.F., Wu, H., Han, X., Li, Q., Gao, Y., Li, Q., Hou, Z., Maruyama, T., Zhang, J., Wang, J., 2015. Toxic role of prostaglandin E < inf > 2 < /inf > receptor EP1 after intracerebral hemorrhage in mice. Brain Behav. Immun. 46, 293–310.

Zhou, K., Enkhjargal, B., Xie, Z., Sun, C., Wu, L., Malaguit, J., Chen, S., Tang, J., Zhang, J., Zhang, J.H., 2018. Dihydrolipoic acid inhibits lysosomal rupture and NLRP3 through lysosome-associated membrane protein-1/calcium/calmodulin-dependent protein kinase II/TAK1 pathways after subarachnoid hemorrhage in rat. Stroke 49, 175–183.